# Carotid-cavernous Fistulas: Diagnosis with Spiral CT Angiography

Oguzhan Coskun, Michèle Hamon, Guillaume Catroux, Lydie Gosme, Patrick Courthéoux and Jacques Théron

*AJNR Am J Neuroradiol* 2000, 21 (4) 712-716
http://www.ajnr.org/content/21/4/712

*AJNR Am J Neuroradiol* 21:712–716, April 2000

**Case Report**

# Carotid-cavernous Fistulas: Diagnosis with Spiral CT Angiography

Oguzhan Coskun, Michèle Hamon, Guillaume Catroux, Lydie Gosme, Patrick Courthéoux, and Jacques Théron

**Summary: Four cases in which the diagnosis of carotid-cavernous fistula was made by using CT angiography are illustrated. The diagnosis was confirmed by digital subtraction angiography in all four instances. To our knowledge, this is the first report of the CT angiographic appearance of carotid-cavernous fistulas.**

Advances in spiral CT coupled with continuing progress in 3D imaging have resulted in exciting new applications for CT. In neuroradiology, these techniques can aid in the diagnosis and therapeutic planning of diseases of the neck vessels (1–3) and of intracranial aneurysms (4, 5). Developments in CT angiography are especially important because they may replace the more invasive conventional angiographic procedures.

Digital subtraction angiography (DSA) is currently the standard of reference in the diagnosis of dural and direct carotid-cavernous fistulas (CCFs) (6, 7). We report four cases in which the diagnosis of CCF was made using CT angiography and confirmed by catheter angiography. We describe CT angiography and postprocessing techniques with a focus on the use of the volume rendering technique for the assessment of CCF.

## Representative Case Reports and Technique

*Case 1*

Three weeks after ballistic trauma, a 40-year-old man noticed diplopia, chemosis, and exophthalmos. He presented with a right abducens nerve palsy and right ocular hypertension (24 mm Hg). CT angiography revealed an enlarged right cavernous sinus with dilated venous channels, including the intercavernous sinus, basilar plexus, ipsilateral superior ophthalmic vein (SOV), inferior petrosal sinus, sphenoparietal sinus, and paracavernous sinus (Fig 1A, B, D). Angiography revealed a right-sided, direct, high-flow CCF draining into the contralateral cavernous sinus, anteriorly into the SOV and angular vein, and posteriorly into the basilar plexus and inferior petrosal sinus (Fig 1C). Regression of ocular symptoms was obtained after endovascular treatment by transarterial and transvenous embolization.

*Case 2*

A 69-year-old woman was admitted for left-sided exophthalmos, chemosis, and dilated episcleral vessels. CT angiography showed enlarged bilateral cavernous sinuses with a dilated left SOV (Fig 2A, C, D). No other draining venous structures were identified. Angiography confirmed a low-flow dural CCF, fed by bilateral meningeal arteries and the left meningohypophyseal trunk, that drained anteriorly into the left SOV (Fig 2B). This CCF was successfully treated by superselective external carotid arterial embolization.

*Case 3*

A 54-year-old woman was referred for right-sided exophthalmos, chemosis, and dilated episcleral vessels. CT angiography revealed an enlarged enhancing right cavernous sinus, with an irregular lateral wall, suggestive of fistulous dural vessels (Fig 3A and D). Veins drained into the basilar plexus and into the inferior petrosal sinus bilaterally (Fig 3B and C). The SOV was not dilated. Angiography confirmed the dural right CCF, fed by the external carotid artery and the meningohypophyseal trunk of the internal carotid arteries (Fig 3E). Transarterial embolization with glue was performed, supplemented by transvenous embolization of the right cavernous sinus by coils.

*Case 4*

A 79-year-old woman was referred for progressive exophthalmos and ptosis of the left eye. Intraocular pressure of the left eye was 26 mm Hg. CT angiography revealed rapidly enhancing, enlarged, bilateral cavernous sinuses, with an enlarged left SOV, and a large well-opacified basilar plexus (Fig 4A). Angiography confirmed a dural CCF at low flow, fed by the internal and external right carotid arteries (via the meningohypophyseal trunk and the middle meningeal artery, respectively), that drained anteriorly into the left SOV and posteriorly into the right part of the basilar plexus (Fig 4B). The patient was first treated conservatively with manual compression of the carotid arteries. Ocular symptoms, however, worsened and an intraarterial embolization was performed (the feeding branches of the right external carotid artery were embolized superselectively), resulting in partial obliteration of the fistula, with improvement of the symptoms. Three weeks later, the patient presented with an increase in the left exophthalmos, and, more important, an increase in intraocular pressure (60 mm Hg). CT angiography showed no enhancement of the left cavernous sinus and partial enhancement of the SOV, suggestive of partial thrombosis, and an enlarged right enhancing cavernous sinus (Fig 4C). These findings were confirmed by angiography, which depicted opacification of the intercavernous sinus (Fig 4D). Clinical improvement occurred after systemic heparinization.

*Technique*

Spiral CT was performed with a Picker PQ 5000 scanner (Picker International, Highland Heights, OH). Patients were placed in the supine position, and a lateral scout image was acquired. Scanning started at the skull base and proceeded caudocranially. A total of 100 mL of nonionic contrast material (Xenetix 300, Guerbet Laboratories, Aulnay-sous-Bois,

Received July 16, 1999; accepted after revision October 27.

From the Department of Neuroradiology and Interventional Radiology, Centre Hospitalo-Universitaire, Avenue Côte de Nacre, 14033 Caen, France. Address reprint requests to Michèle Hamon, MD.

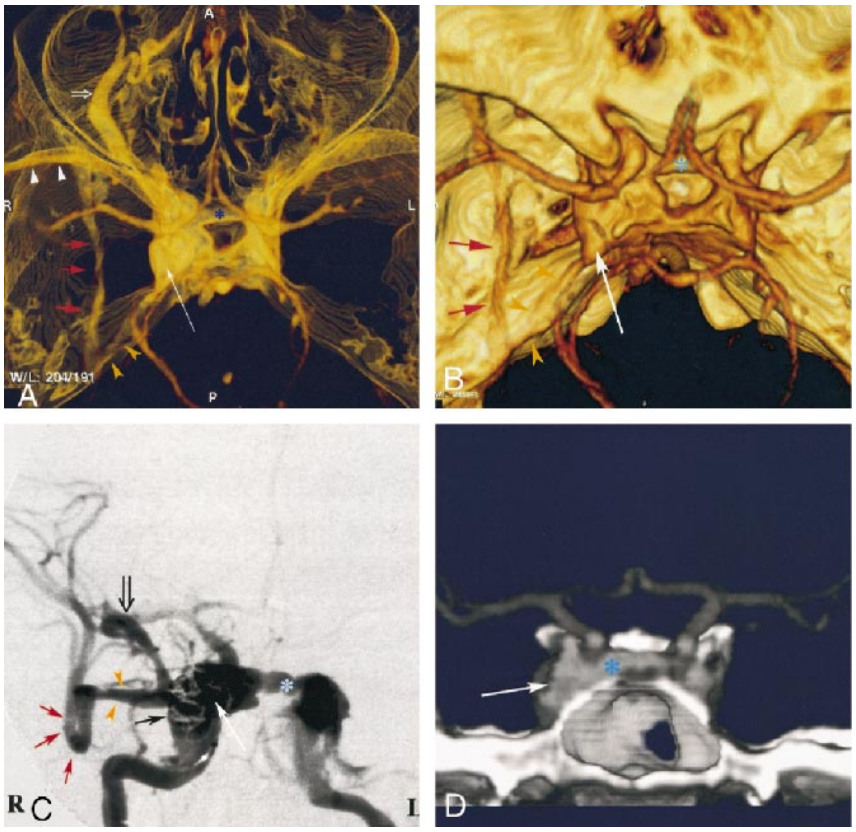


FIG 1. Case 1: 40-year-old man with direct, posttraumatic, right-sided CCF.

*A* and *B,* Superior view of 3D CT angiogram obtained with the volume rendering technique shows an enlarged right cavernous sinus (*long arrow*) with several draining veins: large right SOV (*open arrow, A*), anterior intercavernous sinus (*asterisk*), inferior petrous sinus (*yellow arrowheads*), sphenoparietal sinus (*white arrowheads, A*), and paracavernous sinus (*red arrows*).

*C,* DSA during embolization with selective right internal carotid artery injection shows right cavernous fistula with very high flow and multiple venous drainage channels, including large right SOV (*open arrow*), anterior intercavernous sinus (*asterisk*), sphenoparietal sinus (*yellow arrowheads*), and paracavernous sinus (*red arrows*). *Closed black arrow* indicates GDC coils; *long white arrow,* right cavernous sinus.

*D,* Coronal view of 3D CT angiogram obtained with the volume rendering technique, using anterior cutting, clearly depicts intercavernous sinus (*asterisk*). *Arrow* indicates right cavernous sinus.

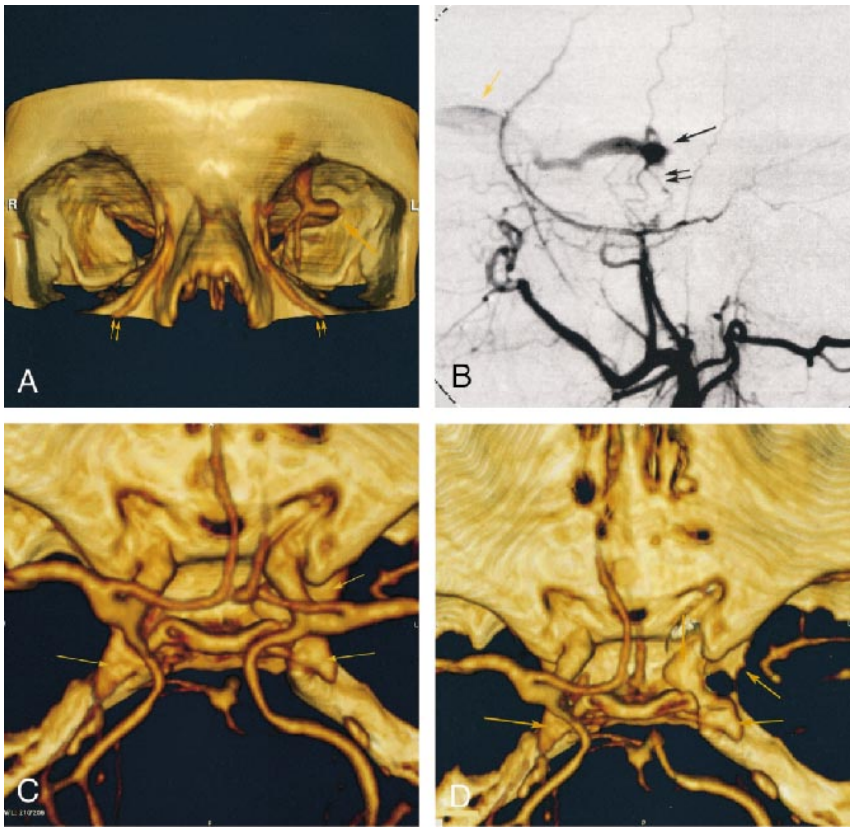


FIG 2. Case 2: 69-year-old woman with dural cavernous fistula.

*A,* Frontal view of 3D CT angiogram obtained with the volume rendering technique shows an enlarged left SOV at the superior orbital fissure (*single arrow*) and dilated angular veins (*double arrows*) bilaterally.

*B,* DSA (selective left external carotid injection, arterial phase, lateral view) shows rapid opacification of a portion of the cavernous sinus (*single black arrow*) supplied by middle meningeal artery branches (*double black arrows*) and draining anteriorly into an enlarged left SOV (*yellow arrow*).

*C,* 3D CT angiogram obtained with the volume rendering technique (superior view) shows bilateral enlarged cavernous sinuses (*arrows*).

*D,* CT angiogram (superior view) better depicts the prominent left cavernous sinus (*arrows*) after cutting to exclude supracavernous internal carotid artery.

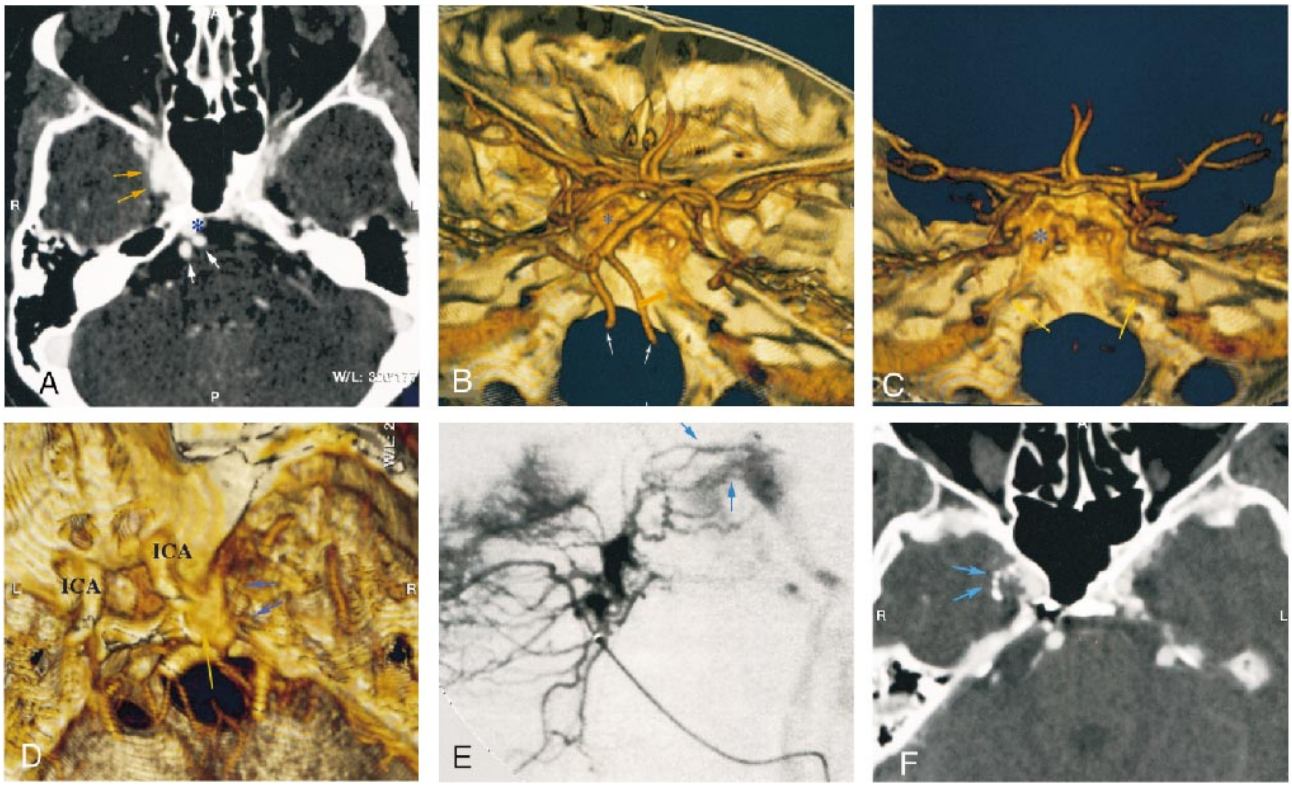


FIG 3. Case 3: 54-year-old woman with dural CCF and right exophthalmos, chemosis, and dilated episcleral vessels.

*A,* CT angiogram (axial source image) shows an enlarged right cavernous sinus with irregular wall (*yellow arrows*) and large ipsilateral basilar plexus (*asterisk*). *White arrows* indicate vertebral arteries.

*B* and *C,* Superolateral (*B*) and posterior (*C*) views of 3D CT angiogram obtained with the volume rendering technique show inferior petrosal sinuses along the posterior surface of the petrous bone (*yellow arrows*). Note the good delineation of skull and vascular anatomy. *Asterisk* indicates basilar plexus; *white arrows,* vertebral arteries.

*D–F,* Superolateral view of 3D CT angiogram obtained with the volume rendering technique (*D*) shows enlarged cavernous sinus (*yellow arrow*). Small vessels (*blue arrows*) might correspond to arteriovenous shunts, well depicted by lateral selective internal maxillary injection on DSA (*E*). CT angiogram (axial source image) after superselective intraarterial embolization shows *n*-butyl cyanoacrylate in these arterial feeders (*F*).

France) was administered at a rate of 3 mL/s by using a power injector and a 20-gauge intravenous catheter inserted into an antecubital vein. Spiral acquisition (1.5-mm collimation, 1.25 pitch, 240-mm field of view, 120 Kv, 150 mA, 512 × 512 matrix) was started 12 seconds after the start of the injection. No test bolus of contrast material was administered to time the acquisition. The images were reconstructed at 1-mm increments by using a 360° linear interpolation algorithm. The window level was at 150 to 200 HU, with a width of 400 to 700 HU. CT data were transferred to an independent workstation (Vitrea workstation; Vital Images Inc., Fairfeild, IA). Three-dimensional reconstructions were performed using the volume rendering technique. Postprocessing required 10 to 15 minutes in each case.

Conventional angiograms were obtained on a digital subtraction system (Digitron, Siemens, Iselin, NJ) by using a femoral approach, and selective catheterization of the internal and external carotid arteries was performed.

## Discussion

CCFs are classified into dural and direct types. A traumatic CCF often has a single direct communication between the internal carotid artery and the cavernous sinus, and corresponds to a direct CCF. In other cases, occurring most often in middle-aged women, there are multiple dural feeders and numerous microfistulas within the cavernous sinus wall; these lesions are often spontaneous and unrelated to trauma. CCF usually presents with neuro-ophthalmologic symptoms that include proptosis, chemosis, cranial nerves palsies (III, IV, V, and VI; partial or complete) and dilated episcleral veins (6).

With direct or dural CCFs, the venous drainage may be multidirectional (Fig 5): 1) *Anterior*—drainage to the ophthalmic venous system produces proptosis, chemosis, and dilated conjunctiva; the blood flow is toward the facial venous system and external jugular vein. 2) *Posterior*—the fistula may drain into the superior petrosal sinus, the inferior petrosal sinus, or the basilar plexus. 3) *Lateral*—drainage is to the sphenoparietal sinus. 4) *Contralateral*—both cavernous sinus plexus anastomose anteriorly and posteriorly via the intercavernous sinus. 5) *Inferior*—usually of minor importance; flow can be into the pterygoid plexus via the vein of the foramen rotundum and the vein of the foramen ovale. Most often, the direction of drainage is mixed.

DSA is currently the standard of reference for the diagnosis of dural and direct CCFs; however,

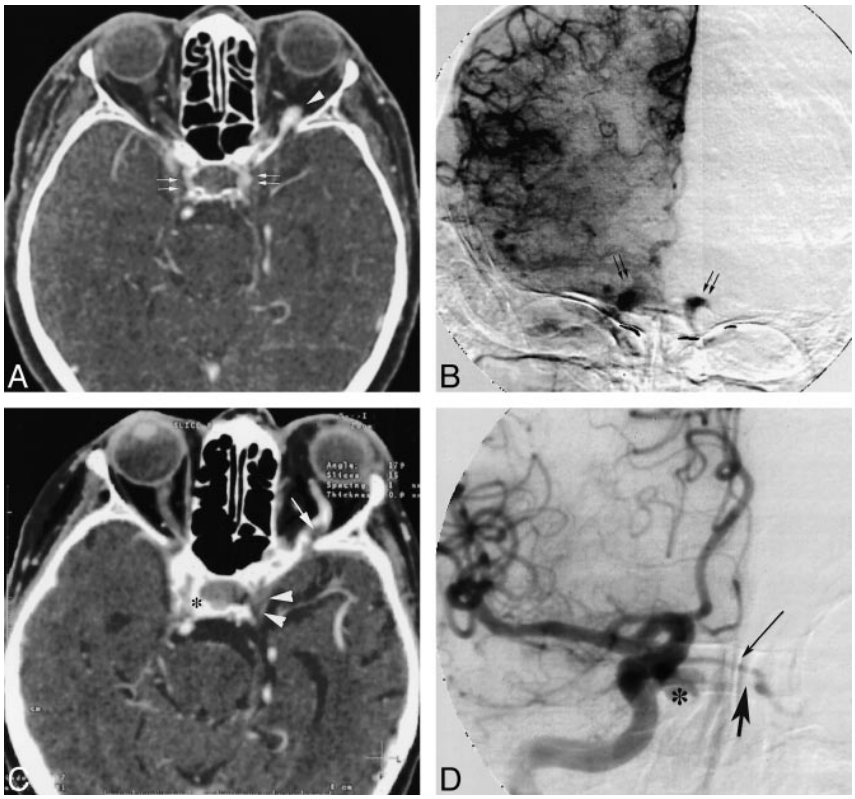


FIG 4. Case 4: 69-year-old woman with a dural fistula involving bilateral cavernous sinuses.

*A,* CT angiogram (axial source image) shows enhancement of bilateral cavernous sinuses (*double arrows*) and enlarged left SOV (*arrowhead*).

*B,* DSA (right common carotid injection, late arterial phase, anteroposterior view) shows early opacification of bilateral enlarged cavernous sinuses (*arrows*).

*C,* CT angiogram (axial source image), after partial embolization, shows partial thrombosis of left SOV (*arrow*), without enhancement of left cavernous sinus (*arrowheads*), and persistent right enlarged cavernous sinus (*asterisk*).

*D,* DSA (right common carotid injection, arterial phase, anteroposterior view) confirms rapid opacification of right cavernous sinus (*asterisk*) and intercavernous sinus (*thin arrow*), without enhancement of left cavernous sinus (*thick arrow*).

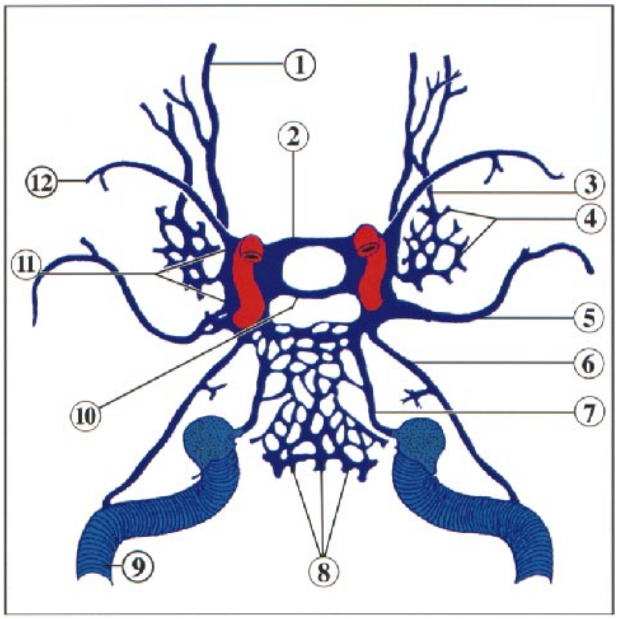


FIG 5. Schematic anatomic diagram of the venous vasculature of the skull base (superior view). *1,* superior ophthalmic vein; *2,* anterior intercavernous sinus; *3,* inferior ophthalmic vein; *4,* pterygoid plexus; *5,* middle meningeal vein; *6,* superior petrosal sinus; *7,* inferior petrosal sinus; *8,* basilar venous plexus; *9,* transverse sinus; *10,* posterior intercavernous sinus; *11,* cavernous sinus; *12,* sphenoparietal sinus.

recent developments in noninvasive techniques, such as spiral CT, have provided useful new tools for the early and safe diagnosis of these vascular disorders. To our knowledge, no report has described the spiral CT angiographic findings in the diagnosis of CCF.

In our limited series, all cases were accurately detected on spiral CT scans. CT angiography showed an enlarged enhancing cavernous sinus at the arterial phase. Scan delay (12 seconds) was chosen to obtain optimal arterial enhancement, based on previous studies evaluating the circle of Willis and the detection of aneurysms. Bonneville (8), in a large series (680 patients), showed that optimal enhancement of the laterosellar veins occurs 5 seconds after optimal enhancement of the internal carotid; and 10 seconds later, the cavernous sinus becomes homogeneous.

CT angiography depicts certain draining veins very clearly (eg, an enlarged SOV could be identified in three of our patients), and other venous drainage channels can also be recognized, such as the intercavernous sinus, basilar plexus, petrosal sinus, sphenoparietal sinus, and paracavernous sinus (9).

Image reconstruction and manipulation were performed on a Vitrea workstation. Many postprocessing techniques, such as multiplanar reformatting, shaded surface displays, maximum intensity projections, and volume rendering, were available. In our experience, the volume rendering technique provides better image reliability and is the most helpful in the evaluation of CCF. Inspection of the axial source images, however, remains an essential part of the assessment (Fig 3A and F). The major difficulties in the exploration of CCFs are related to the proximity between bone and skull base. With

the volume rendering algorithm, lower attenuation voxels (ie, parenchymal brain and CSF) can be excluded, yielding images of vessels and other high-attenuation structures, such as bone. Unlike the maximum intensity projection and surface rendering techniques, which display only approximately 10% of the entire data, the volume rendering method uses the entire data set. Moreover, it provides a more realistic 3D appearance and depicts anatomic relationships more accurately. Surface rendering is not optimal for visualization of structures that do not have naturally well-differentiated surfaces, such as vessels and bone at the skull base. The volume rendering technique can display the bony structures and the vasculature separately, and is particularly useful for visualizing multiple overlapping vessels and locating vessels relative to osseous structures (10, 11). The 3D images are rendered and displayed in real time. Clip planes can be applied to cut a slab of data from the volume in an orientation chosen by the user, so the use of clip planes enables visualization of structures that would otherwise be obscured (Figs 1D and 2D).

Nonetheless, CT angiography has some limitations in the evaluation of CCF. Despite its ability to reliably delineate certain draining veins, it rarely depicts small feeding arteries in dural CCFs or the exact site of fistulous communication in direct CCFs. Moreover, this technique cannot provide information about the blood-flow characteristics within the fistulas.

## Conclusion

Spiral CT angiography seems to be a reliable first-line diagnostic tool in evaluating the presence of a CCF in a suggestive clinical context, and to offer an accurate and safe method for noninvasive and reproducible follow-up. Because of its lower spatial resolution, however, spiral CT angiography is unable to depict the topography of the shunt in traumatic CCFs or the feeding branches in dural arteriovenous malformations. Therefore, it cannot replace conventional angiography, which is always needed to investigate feeding pedicles and venous drainage routes for planning endovascular interventional treatment. Further studies, with larger groups, are required to determine the exact role of CT angiography in the evaluation of CCF.

## References


1. Leclerc X, Godefroy O, Pruvo JP, Leys D. **Computed tomographic angiography for the evaluation of carotid artery stenosis.** *Stroke* 1995;26:1577–1581
2. Simonetti G, Bozzao A, Floris R, Silvestrini M. **Non-invasive assessment of neck-vessel pathology.** *Eur Radiol* 1998;8: 691–697
3. Leclerc X, Godefroy O, Lucas C, et al. **Internal carotid arterial stenosis: CT angiography with volume rendering.** *Radiology* 1999;210:673–682
4. Schwartz RB, Tice HM, Hooten SM, Hsu L, Stieg PE. **Evaluation of cerebral aneurysms with helical CT: correlation with conventional angiography and MR angiography.** *Radiology* 1994; 192:717–722
5. Alberico RA, Patel M, Casey S, Jacobs B, Maguire W, Decker R. **Evaluation of the circle of Willis with three-dimensional CT angiography in patients with suspected intracranial aneurysms.** *AJNR Am J Neuroradiol* 1995;16:1571–1578
6. Lasjaunias P, Berenstein A, eds. ***Surgical Neuroangiography.*** New York: Springer; 1987:;2: 175–211, and 8:274–315
7. Halbach V, Higashida R, Hieshima G, Reicher M, Norman D, Newton T. **Dural fistulas involving the cavernous sinus: results of treatment in 30 patients.** *Radiology* 1987;163:437–442
8. Bonneville JF, Cattin F, Racle A, et al. **Dynamic CT of the laterosellar extradural venous spaces.** *AJNR Am J Neuroradiol* 1989;10:535–542
9. Theron J. **Les affluents du plexus caverneux.** *Neurochirurgie* 1972;18:623–638
10. Kuszyk B, Heath D, Ney D, et al. **CT angiography with volume rendering: imaging findings.** *AJR Am J Roentgenol* 1995;165: 445–448
11. Johnson P, Heath D, Kuszyk B, Fishman. **CT angiography: thoracic vascular imaging with interactive volume rendering technique.** *J Comput Assist Tomogr* 1997;21:110–114